

A Calibration-Independent Technique of Measuring Soot by Laser-Induced Incandescence Using Absolute Light Intensity*

David R. Snelling, Gregory J. Smallwood, Ömer L. Gülder, and Fengshan Liu

*National Research Council Canada
ICPET, Combustion Research Group, Bldg. M-9
Montreal Road, Ottawa, Ontario K1A 0R6, Canada*

and

William D. Bachalo

*Artium Technologies
14660 Saltamontes Way
Los Altos Hills, CA 94022-2036, USA*

ABSTRACT

Laser-induced incandescence (LII) has been proven to be a useful diagnostic tool for spatially and temporally resolved measurement of particulate (soot) mass and volume fraction, and primary particle size in a wide range of applications such as steady flames, flickering flames, and diesel engine exhausts. In this technique, a high-energy pulsed laser is used to rapidly heat the soot particles in the measurement volume to temperatures significantly above the local flame temperature. Analysis of the incandescence signals emitted by the heated soot particles yields information on the local soot volume fraction and the primary particle size. To make quantitative measurements of concentration there is a need for a calibration. Conventionally, the calibration is performed in a source of particles with a known particle volume fraction or particle concentration. This paper presents a novel technique for the determination of soot volume fraction by LII using absolute light intensity measurements, avoiding the need for a source of particles with a known soot volume fraction, and thus extending the capabilities of LII for making practical quantitative measurements of soot. The sensitivity of the detection system is determined by calibrating with an extended source of known radiance and then this sensitivity is used to interpret the measured LII signals. Although it requires knowledge of the soot temperature, either from a numerical model of soot particle heating or experimental observation of the soot temperature, this approach offers a calibration independent technique for measuring soot volume fraction by LII.

* The Second Joint Meeting of the US Sections of the Combustion Institute, Oakland, California, March 25-28, 2001

NOMENCLATURE

Upper-case:

<i>A</i>	area (m ²)
<i>AP</i>	aperture
<i>C₁</i>	first radiation constant (3.7417749·10 ⁻¹⁶ W·m ²)
<i>C₂</i>	second radiation constant (0.01438769 m·K)
<i>E(m)</i>	refractive index dependent function; $E(m) = \text{Im}((m^2-1)/(m^2+2))$
<i>F</i>	fluence (J/cm ²)
<i>M</i>	magnification
<i>P</i>	power (W)
<i>PS</i>	spectral power (W/nm)
<i>PT</i>	total power (W)
<i>R</i>	spectral radiance (W/m ² ·sr·nm)
<i>S</i>	source
<i>T</i>	temperature (K)
<i>V</i>	photodetector signal (V)

Lower-case:

<i>c</i>	speed of light (2.99792458·10 ⁸ m/s)
<i>d</i>	primary particle diameter (nm)
<i>f_V</i>	volume fraction (ppm)
<i>h</i>	Planck's constant (6.6260755·10 ⁻³⁴ J·s)
<i>k</i>	Boltzmann's constant (1.380658·10 ⁻²³ J/K)
<i>m</i>	refractive index
<i>n</i>	number density (1/m ³)
<i>q</i>	energy (J)
<i>t</i>	time (ns)

<i>u</i>	object distance (m)
<i>v</i>	image distance (m)
<i>w</i>	width (m)
<i>x, y, z</i>	Cartesian coordinates (m)

Greek symbols:

Δ_f	filter bandwidth (nm)
ϵ	emissivity
λ	wavelength of light (nm)
τ	filter transmission
η	calibration factor (W/V)

Subscripts:

<i>AP</i>	aperture
<i>AV</i>	average
<i>B</i>	brightness
<i>c</i>	centre
<i>CAL</i>	calibration
<i>EXP</i>	experimental
<i>f</i>	filter
<i>L</i>	lens
<i>max</i>	maximum
<i>p</i>	particle
<i>S</i>	source
<i>TOT</i>	total
<i>V</i>	volume

INTRODUCTION

The presence of particulate matter, such as soot particles, in the environment has brought about an increased interest in the development of methods and devices for the determination of particulate concentration. The emission of soot from engines, power generation facilities, incinerators, or furnaces, for example, represents a loss of useful energy and further is a serious environmental pollutant and a health risk. However, the presence of soot in flames can also have positive effects. For example, the energy transfer from a combustion process is largely facilitated by the radiative heat transfer from soot.

To develop processes and techniques for limiting the emission of soot, we must first possess suitable means for reliably measuring various soot-related parameters. These methods must have adequate dynamic range in order to be able to monitor and characterize the pollutant emissions over a very wide range of concentrations and must operate under a range of environmental

conditions from *in situ* exhaust to atmospheric monitoring. In the case of particulate matter, information on the particle mass, size, and volume fraction is needed. The lack of availability of suitable diagnostics has resulted in a degree of uncertainty in the correlation of the particulate loading with health effects. Improvements in the instrumentation are needed to help in developing the test protocols, standards and regulations that will preserve the environment and limit risks to health. A need for a reliable soot aerosol measurement technique has been further demonstrated by recent studies showing that soot aerosols in the atmosphere may be the second most important component of global warming after CO₂ (thus, exceeding the direct radiative forcing of CH₄) (Hansen et. al. 2000, Jacobson 2001).

Laser-induced incandescence (LII) measurement is an emerging technology that promises to be a reliable means for spatially and temporally measuring the soot volume fraction and primary soot particle size. Eckbreth (1977) recognized the concept while working with Raman spectroscopy in flames and was troubled by the presence of soot particles that produced laser-modulated incandescence, which could overwhelm the desired Raman signals. He was able to relate the time dependence of this interference to laser particulate heating, heat transfer to the medium, particle vaporization, and indirectly to the particle size. Melton (1984) performed numerical calculations to investigate the possibility of developing a soot diagnostic based on this laser heating of particles. He concluded that it might be possible to obtain the particle temperature, soot primary particle size distribution parameters, and relative soot volume fraction. Dasch (1984) modeled the vaporization of small soot particles and conducted experiments demonstrating the method. Since that time, a number of research teams have investigated the method with varying degrees of success (Bengtsson and Alden, 1989; Dec *et al.*, 1991; Quay *et al.*, 1994; Vander Wal and Weiland, 1994; Bengtsson and Alden, 1995; Will *et al.*, 1995; Mewes and Seitzman, 1997; Snelling *et al.*, 1997; Witze *et al.*, 2001). Dec *et al.* (1991) used the incandescence method to visualize the soot production inside a diesel engine.

With the LII method, the soot within the laser beam path is heated rapidly using a pulsed laser source with duration typically less than 20 ns (FWHM). The soot is heated from the local ambient soot temperature to the soot vaporization temperature (approximately 4000 to 4500 K). The incandescence from the soot particles is measured using collection optics and photodetectors. Using appropriate calibration and analysis of the incandescence signal, information on the soot volume fraction and primary soot particle size may be obtained. Laser energy absorption by the soot particles and the subsequent cooling processes involve complex analysis of the nano-scale heat and mass transfer in time and space. The method is essentially nonintrusive and is capable of making *in situ* measurements over a very large range of soot concentrations in both flames and under ambient conditions. However, it is not completely non-perturbing as the laser heating can be expected to affect the soot morphology (Vander Wal *et al.*, 1998) and cause some evaporation during the short duty cycle of the laser.

LII can fill the need for soot particulate measurements since the LII signal is proportional to a particulate volume fraction over a wide dynamic range. However, LII provides a relative measure of soot concentrations and requires a calibration for quantification of soot particulate concentrations. Currently, calibration of the technique for absolute soot particulate concentrations may be made by *in situ* comparison of the LII signal to a system with a known soot volume fraction determined through traditional methods. An example is shown in Fig. 1,

where the LII signals across the diameter of a laminar diffusion flame are area normalized to the soot volume fraction determined using two-dimensional line-of-sight attenuation (Snelling *et al.*, 1999). Using this empirical calibration procedure LII has been used to measure soot particle volume fraction in steady-state and time-varying diffusion flames, premixed flames and within engines and in engine exhaust streams. In this paper we present a novel technique to perform absolute light intensity measurements in LII avoiding the need for a calibration in a source of soot particulates with a known concentration (Snelling *et al.* 2000a), and thus extending the capabilities of LII for making practical quantitative measurements of soot.

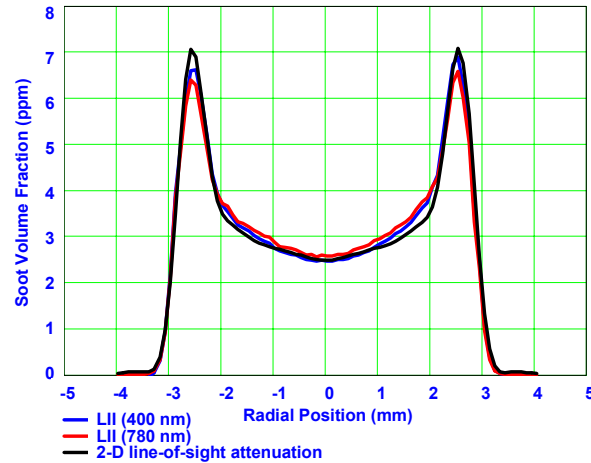


Fig. 1. Example of conventional LII calibration by comparison with known soot concentration in a laminar diffusion flame.

CALIBRATION-INDEPENDENT TECHNIQUE

The soot concentration can be determined by measuring the absolute LII signal, and compare that to the calculated theoretical radiation per particle to calculate the concentration of soot particles. A strip filament lamp whose brightness temperature is known is used to calibrate the detection system. Errors associated with uncertainties in the filter characteristics, lens collection efficiency, aperture size, and optical system magnification are shown to be largely eliminated using this calibration procedure. In a variant of this approach the soot particle surface temperature is measured by recording two or more LII wavelengths simultaneously and using the ratio of these signals to obtain an experimental temperature. The experimental temperature can then alternatively be used to calculate the radiation per particle. From the measured absolute LII signal intensity and the calculated particle radiation intensity the number of particles can then be calculated.

Calibration Set-up

The optical set-up for the calibration is shown schematically in Fig. 2. A calibrated strip filament lamp is placed so that its filament is coincident with the LII signal generation region. The lamp, whose filament is 3x8 mm, has a known brightness temperature (at 654 nm) as a function of lamp current. The filament is imaged with a lens onto an aperture in front of the

photomultiplier. Several optical arrangements have been implemented, including both direct optical coupling and fibre optic coupling, and magnifications of 0.5 and 1.0. Typical aperture dimensions are 1.0 mm diameter, and a typical lens would be 190 mm focal length and 54 mm diameter.

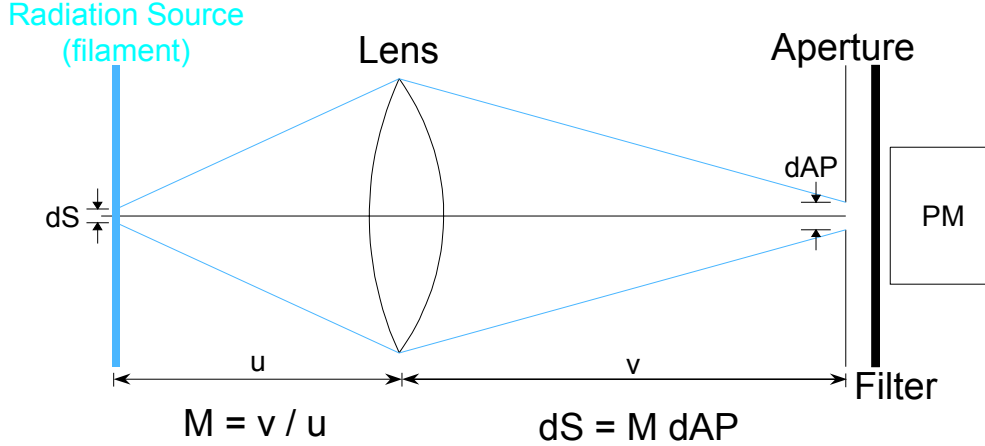


Fig. 2 Optical schematic for absolute intensity calibration.

Calibrated Lamp Signal

The spectral radiance of the lamp (the power emitted per unit area, per unit solid angle, and per unit wavelength interval) is given by:

$$R_s(\lambda) = \frac{2c^2 h \varepsilon(\lambda, T)}{\lambda^5} \left(e^{\frac{hc}{k\lambda T}} - 1 \right)^{-1} = \frac{C_1 \varepsilon(\lambda, T)}{\pi \lambda^5} \left(e^{\frac{C_2}{\lambda T}} - 1 \right)^{-1} \quad (1)$$

where $C_1 = 3.74177 \times 10^{-16} \text{ W}\cdot\text{m}^2$ and $C_2 = 0.014388 \text{ m}\cdot\text{K}$ are the first and second radiation constants, and $\varepsilon(\lambda, T)$ is the emissivity as a function of wavelength and temperature.

The calibrated lamp has a known brightness temperature T_B (temperature at which a perfect black body would emit the same amount of radiation) at 654 nm from which the true filament temperature (T_S) can then be obtained from:

$$T_S = \left(\frac{1}{T_B} + \frac{\lambda}{C_2} \cdot \ln(\varepsilon(\lambda, T_S)) \right)^{-1} \quad (2)$$

since the exponential term $\gg 1$ in Eq. 1, for the temperatures and wavelengths considered here. With the known emissivity of tungsten (Pon and Hessler, 1984) as a function of temperature and wavelength the filament radiance can be obtained at any desired wavelength from Eq. 1. The filament radiant power incident on the detector is given by:

$$P_{CAL} = M^2 A_{AP} \frac{A_L}{u^2} \int_{\lambda} R_s(\lambda) \tau(\lambda) d\lambda \quad (3)$$

where A_{AP} is the area of the aperture, $\tau(\lambda)$ is the filter transmission as a function of wavelength, and u and M are defined in Fig. 2. The observed signal, V_{CAL} , from the calibration lamp then provides a detection system calibration factor $\eta = P_{CAL}/V_{CAL}$.

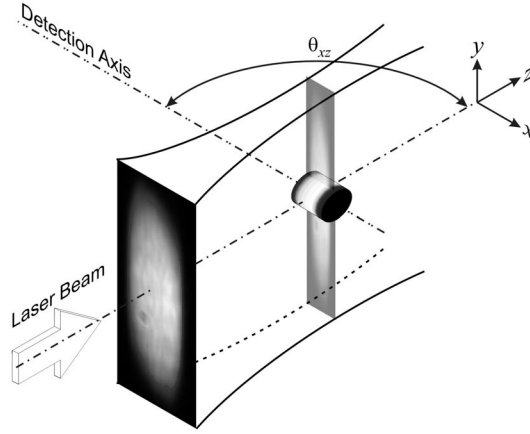


Fig. 3. Schematic illustrating laser mini-sheet with near-top-hat spatial fluence distribution over sample volume.

Theoretical LII Intensity

Using the calibration factor defined above, the observed LII photomultiplier signals can be converted to a detected intensity. We can now compare this observed signal with that calculated by the LII model. The volume of the heated soot particle imaged onto the detector is defined by a cylinder with a cross-sectional area $M^2 \cdot A_{AP}$ and with a length equal to the detected beam path length across the thickness of the laser sheet, as shown in Fig. 3. A mini-sheet is employed to minimize the variation in fluence in the y -direction for the detected region. The laser fluence is essentially constant across the elliptical cross-section (depending upon detection angle θ_{xz}) of the cylinder along the path of the laser beam, since only the centre of the laser mini-sheet is viewed, but has a marked dependence along the cylinder axis (i.e., through the laser sheet). The spatial distribution of the fluence of the laser beam ($f(x,y)$) is obtained from a 2D (xy plane) image of the laser beam using a CCD camera, where the dimension orthogonal to the sheet is x and the laser beam propagation direction is z . The mean fluence along the x -axis ($F(x)$) is readily calculated by integrating $f(x,y)$ over the viewed cross section. This mean fluence, $F(x)$, is conveniently normalized for unit total laser energy and can then be scaled by q_{TOT} to obtain the distribution for other laser energies.

For a given single particle we calculate the total LII spectral power (PS_p) (i.e. power/unit wavelength) radiated into 4π steradians. PS_p is a function of laser fluence, wavelength, and time (and to a lesser extent of gas temperature and laser pulse duration). The theoretical LII power (P_p) for a single particle corresponding to the experimental detection conditions is then:

$$P_p(F, t) = \frac{A_L}{4\pi u^2} \int_{\lambda} PS_p(F, \lambda, t) \tau(\lambda) d\lambda \quad (4)$$

where $A_L/4\pi u^2$ is the fraction of the total radiation collected by the lens. For a soot particle number density n_p we can now calculate the theoretical total power (PT_p) that would be observed in the experiment by integrating $PS_p(F)$ over the region of space that is imaged onto the detector.

$$PT_p = n_p M^2 A_{AP} \frac{A_L}{4\pi u^2} \int_{\lambda} \int_x PS_p(F(x), \lambda, t) \tau(\lambda) d\lambda dx \quad (5)$$

Variation of soot particle concentration in the observation region has been ignored.

Comparison of Theory to Experiment

The experimentally observed LII signal voltage, V_{EXP} , can be converted to power using the system calibration, η , defined above, i.e., $P_{EXP} = \eta \cdot V_{EXP} = P_{CAL} \cdot V_{EXP}/V_{CAL}$, substituted in Eq. 3, and can then be equated to the theoretical total power in Eq. 5.

$$\frac{V_{EXP}}{V_{CAL}} M^2 A_{AP} \frac{A_L}{u^2} \int_{\lambda} R_S(\lambda) \tau(\lambda) d\lambda = n_p M^2 A_{AP} \frac{A_L}{4\pi u^2} \int_{\lambda} \int_x PS_p(F(x), \lambda, t) \tau(\lambda) d\lambda dx \quad (6)$$

n_p can now be calculated from Eq. 6 since all the other quantities are measured or obtained from theory. It is that the magnification (M), the aperture size (A_{AP}), and the collection solid angle of the lens (A_L/u^2) are common to both sides of Eq. 6 and they cancel out. The calibration is independent of the exact value assumed for these quantities. The integration over the filter bandwidth is also common to both sides and effectively cancels out. Thus the strip filament calibration lamp provides a source of known radiance, which we can compare the soot particle radiation with, independent of any exact knowledge of the filter characteristics, collection solid angle, or viewing region cross-sectional area, provided the calibration source fills the field-of-view of the detection system.

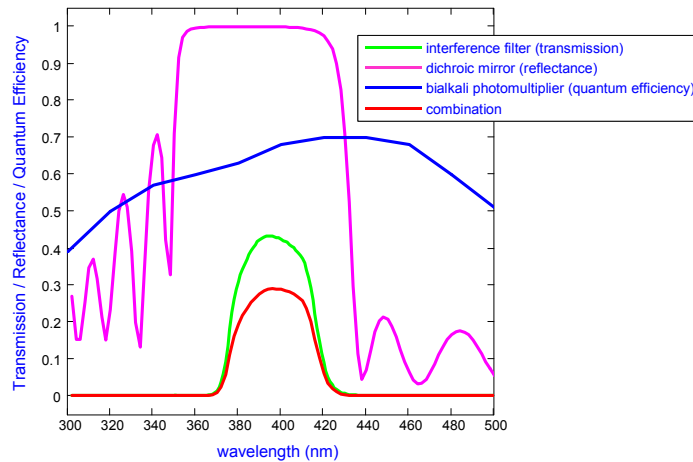


Fig. 4. Example of effective filter transmission for spectrally uniform illumination, incorporating interference filter, dichroic mirror, and photomultiplier characteristics.

The combined filter transmission for our 400 nm detector is shown in Fig. 4. The filter transmission curve used in the integrations over the filter bandwidth in Eq. 6 does not strictly cancel since both the calibration lamp radiance and the LII signals are also functions of

wavelength. However, in practice it has been found that, to a good approximation, the filter transmission curve may be replaced by an equivalent filter with a centre wavelength λ_c , a bandpass Δ_f , and a transmission τ_{max} where the latter is the observed peak transmission of the filter. The equivalent bandpass is given by:

$$\Delta_f = \frac{\int \tau(\lambda) d\lambda}{\tau_{max}} \quad (7)$$

where the integration is over the total filter bandwidth. The centre wavelength, λ_c , is the wavelength limit for which the integral in Eq. 11 is $\frac{1}{2}$ the total integral over all wavelengths. The filter transmission is from $\lambda_c - \Delta_f/2$ to $\lambda_c + \Delta_f/2$. The integrations over the filter bandwidth in Eq. 6 may now be replaced by $\tau_p \cdot \Delta_f \cdot R(\lambda_c)$, where we have used the lamp radiance at the centre of the filter bandwidth. The approximation to the total integral in Eq. 3 and the LHS of Eq. 6 requires a correction of $\sim 12\%$ for a filter with a bandwidth of 40 nm, centred at 400 nm, and a filament temperature of 1600 K, as shown in Fig. 5. This is the maximum correction likely to be encountered in the calibration since the error decreases as the lamp (or particle) temperature and centre wavelength increase. The error involved in similarly replacing the integration in Eq. 4 and the RHS of Eq. 6 is smaller since the variation of LII signal with wavelength is less than that of the calibration lamp due to the higher temperatures. At typical peak laser heated soot particle temperatures the corrections are $< 1\%$. For the lamp calibrations, the error involved in replacing the integration with Eq. 7 is corrected for.

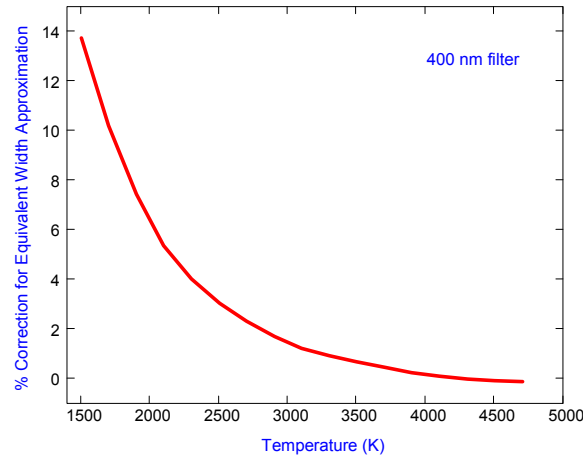


Fig. 5. Correction factor required for substitution of equivalent width in place of the actual spectral filter transmission.

Simplified Calibration Procedure: Method I **Primary Particle Number Density Using Theoretically Derived Particle Intensity**

The cancellation of the magnification, solid angle, and filter transmission in Eq. 6 leads to a considerable simplification. Perhaps, more importantly, it also leads to an important increase in experimental accuracy in that small errors in the measurements of the magnification, solid angle and filter transmission largely cancel because they affect the calibration in the same way they

affect the calculated theoretical intensity. Thus a simplified calibration is now performed where instead of Eq. 3 we merely use the filament radiance at the filter centre wavelength ($R_S(\lambda_c)$).

Eq. 3 becomes

$$P_{CAL} = M^2 A_{AP} \frac{A_L \tau_p \Delta_f}{u^2} R_S(\lambda_c) \quad (3b)$$

The calibration constant η is now calculated using $\eta = R_S(\lambda_c)/V_{CAL}$. The calibration factor η is now in units $W \cdot m^{-2} \cdot sr^{-1} \cdot V^{-1} \cdot \text{unit wavelength interval}^{-1}$ (or $W/V \cdot m^3 \cdot sr$).

Eq. 4 becomes:

$$P_p(F, t) = \frac{A_L \tau_p \Delta_f}{4\pi u^2} PS_p(F, \lambda_c, t) \quad (4b)$$

and the simplified form of Eq. 6 (using Eqs. 3b and 4b) becomes

$$V_{EXP} \cdot \eta = \frac{V_{EXP}}{V_{CAL}} \cdot R_S(\lambda_c) = \frac{n_p}{4\pi} \int_x PS_p(F(x), \lambda_c, t) dx \quad (6b)$$

n_p can be calculated from Eq. 6b. The particle (soot) volume fraction is then given by:

$$f_V = n_p \cdot \frac{\pi d_p^3}{6} \quad (8)$$

Since P_p and thus PS_p are proportional to primary particle volume (i.e. d_p^3) the soot particle volume fraction is independent of the exact value of d_p assumed in Eqs. 6b and 8.

Simplified Calibration Procedure: Method II

Primary Particle Number Density Using Experimentally Derived Particle Temperature

If two or more independent wavelengths are recorded, an average soot particle surface temperature across the laser sheet can be calculated by using the ratio of the observed signals (corrected for detection sensitivity) and the known soot particle absorption cross sections. The power radiated by a single particle of diameter d_p is given by (see, e.g. Snelling *et al.*, 2000b, Smallwood *et al.*, 2001)

$$P_p(\lambda) = \frac{8\pi^3 c^2 h}{\lambda^6} \left(e^{\frac{hc}{k\lambda T}} - 1 \right)^{-1} d_p^3 E(m) \quad (9)$$

where m , the complex refractive index, is a function of wavelength. The ratio of the powers at two wavelengths is then given by

$$\frac{P_p(\lambda_1)}{P_p(\lambda_2)} = \frac{\lambda_2^6}{\lambda_1^6} \frac{\left(e^{\frac{hc}{k\lambda_2 T}} - 1 \right) E(m_{\lambda_1})}{\left(e^{\frac{hc}{k\lambda_1 T}} - 1 \right) E(m_{\lambda_2})} \quad (10)$$

The observed signal ratio at the two wavelengths $V_{EXP}(\lambda_1)/V_{EXP}(\lambda_2)$ can be converted to relative powers (P_{EXP}) using the calibration factors

$$\frac{P_{EXP}(\lambda_1)}{P_{EXP}(\lambda_2)} = \frac{V_{EXP}(\lambda_1)}{V_{EXP}(\lambda_2)} \frac{\eta(\lambda_1)}{\eta(\lambda_2)} \quad (11)$$

Using this experimentally determined power ratio and the known values of $E(m)$, Eq. 10 can be solved for T . In this case it is only the relative, not the absolute, magnitude of the particle absorption cross-section at the two wavelengths that is important in determining soot particle surface temperature. This temperature, derived from a power ratio measurement at two wavelengths, represents some average soot particle surface temperature through the nonuniform laser sheet. The integral in the right hand side of Eq. 6b can now be approximated as

$$P_p(T_{AV}, \lambda_c) \cdot w_x \quad (12)$$

where w_x is the sheet thickness. Eq. 6b becomes:

$$V_{EXP} \cdot \eta = \frac{V_{EXP}}{V_{CAL}} R_S(\lambda_c) = \frac{n_p}{4\pi} P_p(T_{AV}, \lambda_c) w_x \quad (6c)$$

n_p , the primary particle number density, can now be calculated from Eq. 6c since all other quantities are known. As with Method I, the particle (soot) volume fraction is calculated with the formulation presented in Eq. 8, and is independent of the exact value of d_p assumed in Eqs. 6c and 8.

The sheet thickness w_x is obtained by numerical simulation where we use

$$PS_{AV} \cdot w_x = \int_x PS_p(F(x), \lambda_c, t) dx \quad (13)$$

where PS_{AV} is the calculated power for an a particle at the average temperature calculated from the numerical simulation analogously to the experimentally derived mean temperature. Numerical simulation is used to calculate an average sheet width, and the theoretical particle temperatures are not used directly. The sheet thickness is a weak function of fluence but the error involved in using an average value is $< 5\%$, particularly for a near top-hat profile. Eq. 6c is only an approximation since it is not rigorously true that the average temperature can reproduce the absolute radiance. Numerical simulation of this averaging approximation compared to the correct radiant powers indicated that, for a Gaussian profile, it underestimates the power by $\sim 20\%$. The derived soot particle number density derived from the approximation in Eq. 6c will then be $\sim 20\%$ high. In practice using the numerical simulation results to apply an appropriate correction can reduce this error. Numerical simulation also indicates that a laser fluence profile that is closer to “top-hat” (i.e. constant fluence across the laser sheet) will result in much smaller errors.

The average soot particle surface temperature, T_{AV} , can be solved for as a function of time when two or more independent wavelengths are recorded. At some time after the laser excitation, the evaporation diminishes, and conduction to the surrounding gas becomes the dominant cooling mechanism for the particle. During the conduction phase, the difference between the particle surface temperature and the ambient gas temperature decays steadily in an exponential manner.

The time constant of this decay is inversely proportional to d_p , the primary particle diameter (Snelling *et al.* 2000c). Thus this method can provide the size of the primary particles as well as the concentration.

RESULTS

Briefly, examples of the results obtained with the Simplified Calibration Procedure: Method II described above are presented. These results were obtained using a multimode Nd:YAG laser with a near-top-hat spatial profile, two- or three-wavelength detection (only two wavelengths are shown), and detection at 35° off-axis. For further details on the experimental method employed, see, e.g. Snelling *et al.* (2000c). The absolute intensities measured as a function of time are shown in Fig. 6. The peak temperatures recorded for each of these examples is listed in Table 1, along with the soot volume fraction associated with that temperature.

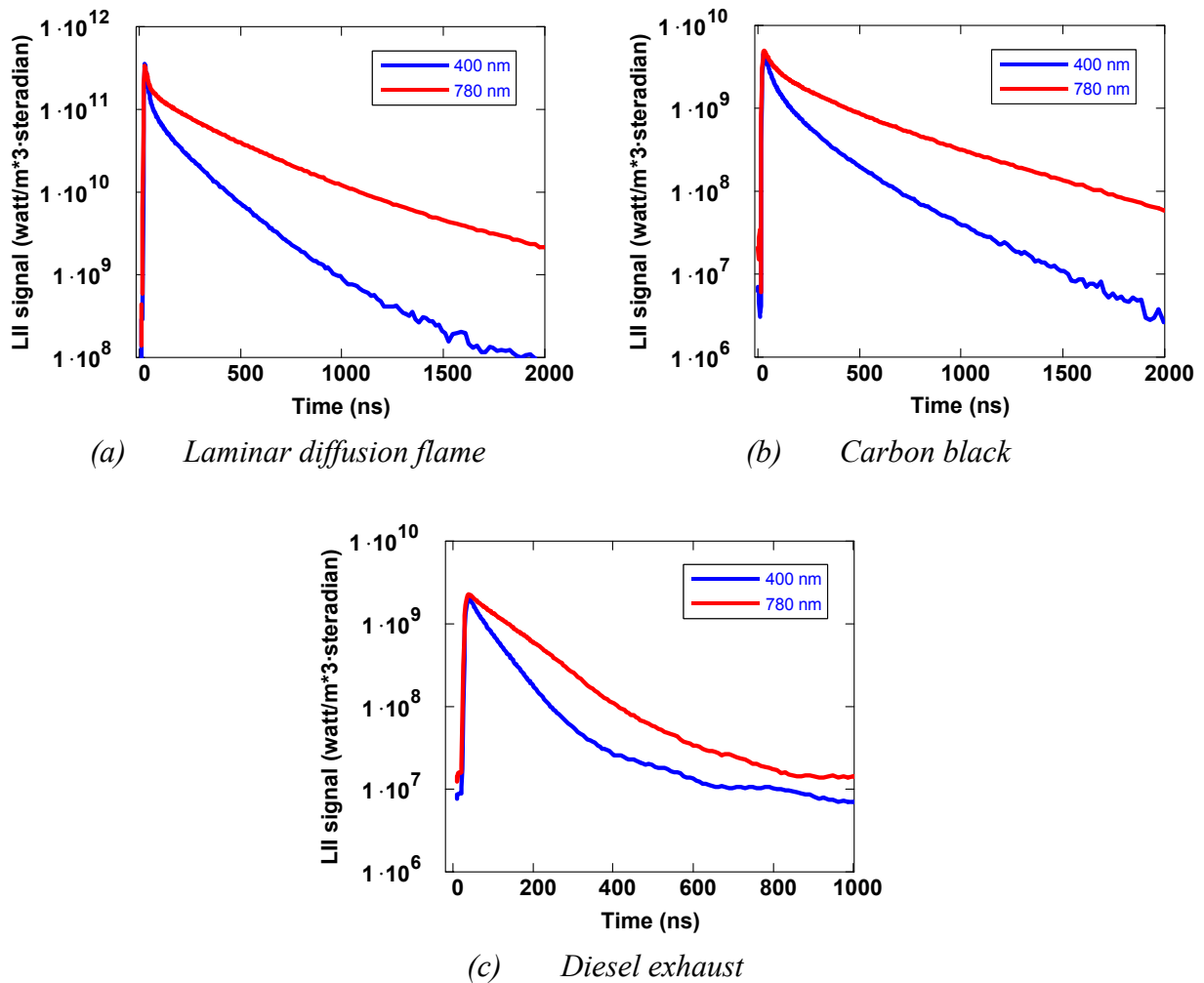


Fig. 6. Examples of absolute intensities recorded at 400 nm and 780 nm in a variety of particulate-laden streams.

Table 1. Measurement Range Achieved with Absolute Intensity Calibration

Application	Peak Temperature*	Soot Volume Fraction*	Measured SVF Range
Laminar Diffusion Flame	4690 K	3.1 ppm	100 ppb – 10 ppm
Carbon Black	4520 K	79 ppb	10 ppb – 100 ppb
Diesel Exhaust (dilute)	4440 K	27 ppb	50 ppt – 50 ppb

* for data shown in Fig. 6

The results of analysis of the data from the laminar diffusion flame are shown in Fig. 7, where the temperature is determined from the absolute intensities at two wavelengths using Eq. 10, and then the soot volume fraction is determined using Eqs. 6c, 8, and 9. The measured soot volume fraction of ~ 3.2 ppm at the time of the peak temperature is in agreement with independent determination of the soot concentration (Snelling *et al.*, 1999). Note that in the first 50 ns, one can observe that the evaporation process is reducing the soot volume fraction. This continues until the temperature drops below ~ 4200 K, at which time the soot volume fraction remains relatively constant at ~ 2.6 ppm until the signal becomes too weak for reliable measurement.

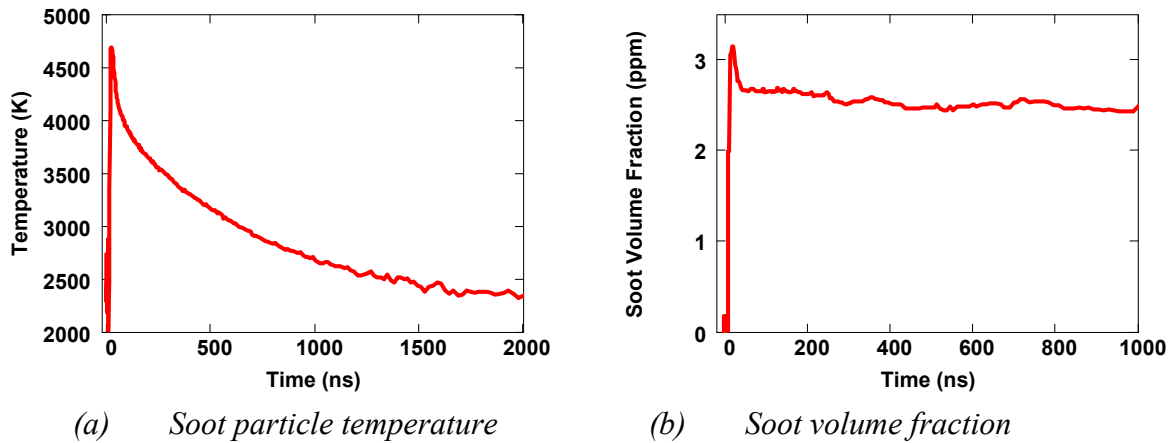


Fig. 7. The soot particle temperature for the data from the laminar diffusion flame shown in Fig. 6(a), and the soot volume fraction determined from the temperature and absolute intensity, both as a function of time.

CONCLUDING REMARKS

A novel technique that provides a method and an apparatus for the determination of soot particle volume fractions with laser induced incandescence using absolute light intensity measurements has been described. This requires knowledge of the soot particle temperature either from a numerical model of particulate heating or experimental observation of the particulate temperature. Further, by using a known soot particle temperature a particle volume fraction is calculated. This avoids the need for a calibration in a source of soot particulates with a known particle volume fraction or particle concentration.

The sensitivity of the detection system is calibrated from an extended source of known radiance and then this sensitivity is used to interpret measured LII signals. This results in a calibration independent method and apparatus for measuring soot particle volume fractions or particle concentrations. A modeling process involves a solution of the differential equations describing the heat/energy transfer of the soot particle and surrounding gas, including parameters to describe vaporization, heat transfer to the medium, particle heating etc. The solution gives temperature and diameter values for the soot particles over time. These values are then converted to radiation values using Planck's equation. Thus, with the present technique there is no need for a source of known soot particulate concentration for calibration purposes, making it useful for practical quantitative measurements.

Two simplified calibration procedures are demonstrated to determine the primary particle number density: one using the theoretically derived soot particle intensity, the other using experimentally derived soot particle temperatures.

ACKNOWLEDGEMENTS

The research performed in Canada was supported by PERD POL 2.1.1 (Particulates), Dr. Keith Puckett, Program Leader. NASA Glenn Research Center supported the research performed in USA.

REFERENCES

- Bengtsson, P. E. and Alden, M., (1989), "Application of a Pulsed Laser for Soot Measurements in Premixed Flames," *Applied Physics B (Photophysics and Laser Chemistry)* B48(2):155-64.
- Bengtsson, P. E. and Alden, M., (1995), "Soot-Visualization Strategies Using Laser Techniques. Laser-Induced Fluorescence in C₂ from Laser-Vaporized Soot and Laser-Induced Soot Incandescence," *Appl. Phys. B: Lasers Opt* 1:51-9.
- Dasch, C. J., (1984), "New Soot Diagnostics in Flames Based on Laser Vaporization of Soot," 20th Symp. (Int.) on Combustion, 1231-1237.
- Dec, J. E., zur Loye, A. O. and Siebers, D. L., (1991), "Soot Distribution in a D.I. Diesel Engine Using 2-D Laser-Induced Incandescence Imaging," *SAE Transactions* 100:277-288.
- Eckbreth, A. C., (1977), "Effects of Laser-Modulated Particulate Incandescence on Raman Scattering Diagnostics," *Journal of Applied Physics* 48(11):4473-4479.
- Hansen, J., Sato, M., Reto, R., Lacis, A., and Oinas, V., (2000), "Global Warming in the Twenty-First Century: An Alternative Scenario," *Proceedings of the National Academy of Sciences* 97:9875-9880.
- Jacobson, M. Z., (2001), "Strong Radiative Heating Due to the Mixing State of Black Carbon in Atmospheric Aerosols," *Nature* 409:695-697.
- Melton, L. A., (1984), "Soot Diagnostics Based on Laser Heating," *Applied Optics* 23(13):2201-2208.
- Mewes, B. and Seitzman, J. M., (1997), "Soot Volume Fraction and Particle Size Measurements with Laser-Induced Incandescence," *Applied Optics* 36(3):709-717.

- Pon, R. M. and Hessler, J. P., (1984), "Spectral Emissivity of Tungsten: Analytic Expressions for the 340-nm to 2.6-micron Spectral Region," *Applied Optics* 23(7):975-976.
- Quay, B., Lee, T. W., Ni, T. and Santoro, R. J., (1994), "Spatially Resolved Measurements of Soot Volume Fraction Using Laser-Induced Incandescence," *Combustion and Flame* 97:3-4.
- Smallwood, G. J., Snelling, D. R., Liu, F. and Gülder, Ö. L., (2001), "Clouds over Soot Evaporation: Errors in Modeling Laser-Induced Incandescence of Soot," *Journal of Heat Transfer*, in press.
- Snelling, D. R., Smallwood, G. J., Campbell, I. G., Medlock, J. E. and Gülder, Ö. L., (1997), "Development and Application of Laser-Induced Incandescence (LII) as a Diagnostic for Soot Particulate Measurements," AGARD Conference Proceedings 598, *Advanced Non-Intrusive Instrumentation for Propulsion Engines*, Brussels, Belgium, 23-1 to 23-9.
- Snelling, D. R., Thomson, K. A., Smallwood, G. J. and Gülder, Ö. L., (1999), "Two-Dimensional Imaging of Soot Volume Fraction in Laminar Diffusion Flames," *Applied Optics* 38(12): 2478-2485.
- Snelling, D. R., Smallwood, G. J. and Gülder, Ö. L., (2000a), "Absolute Light Intensity Measurements in Laser Induced Incandescence," US Patent No. 6,154,277.
- Snelling, D. R., Liu, F., Smallwood, G. J. and Gülder, Ö. L., (2000b), "Evaluation of the Nanoscale Heat and Mass Transfer Model of the Laser-Induced Incandescence: Prediction of the Excitation Intensity," NHTC2000-12132, *Thirty Fourth National Heat Transfer Conference*, Pittsburgh, Pennsylvania.
- Snelling, D. R., Smallwood, G. J., Sawchuk, R. A., Neill, W. S., Gareau, D., Clavel, D., Chippior, W. L., Liu, F., Gülder, Ö. L. and Bachalo, W. D., (2000c), "In-Situ Real-Time Characterization of Particulate Emissions from a Diesel Engine Exhaust by Laser-Induced Incandescence," SAE Paper No. 2000-01-1994.
- Vander Wal, R. L. and Weiland, K. J., (1994), "Laser-Induced Incandescence: Development and Characterization Towards a Measurement of Soot-Volume Fraction," *Applied Physics B* 59:445-452.
- Vander Wal, R. L., Ticich, T. M. and Stephens, A. B., (1998), "Optical and Microscopy Investigations of Soot Structure Alterations by Laser-Induced Incandescence," *Applied Physics B (Lasers and Optics)* B67(1):115-123.
- Will, S., Schraml, S. and Leipertz, A., (1995), "Two-Dimensional Soot-Particle Sizing by Time-Resolved Laser-Induced Incandescence," *Optics Letters* 20(22):2342-2344.
- Witze, P. O., Hochgreb, S., Kayes, D., Michelsen, H. A. and Shaddix, C. R., (2001), "Time-Resolved Laser-Induced Incandescence and Laser Elastic Scattering Measurements in a Propane Diffusion Flame," *Applied Optics*, in press.